



Behaviour and Stability of Double-coped Beam-to-girder Connections under Combined Loading

Graeme Johnston¹, Robert G. Driver², Logan Callele³

Abstract

Removing a portion of the top and bottom flanges of a steel beam, known as coping, is a commonly-used method to eliminate interferences when framing a beam into an equal depth girder. In industrial structures, typically an end-plate is used to bolt the beam end to the girder web. Special attention must be paid to the stability of the coped region due to the reduction in strength and torsional stiffness, but a lack of experimental research on double-coped beams can lead to overly-conservative and costly details. The complexity of the connection behaviour is compounded if axial load is present in addition to shear. An investigation is currently underway into the behaviour and stability of beam-to-girder connections that utilize double-coped beams. Full-scale specimens are tested by rotating the connection by 0.03 radians, a commonly-used value in connection testing that represents a typical beam end rotation at failure under a distributed load, applying an axial load, and then applying a shear load until failure. Axial loads vary between 100 kN in tension and 400 kN in compression. In addition to varying axial loads, the connection support condition, section depth, and cope length were varied to represent geometries found in typical structures that may be susceptible to stability issues. The cope depth was selected as a function of the beam section chosen. Failure modes of the connections are described and the key variables that influence the behaviour and performance of the connection are discussed.

1. Introduction

Often steel framed buildings maintain a constant floor height by constraining the top flanges of beams and supporting girders to be at the same elevation. Removing a portion of the beam flanges, known as “coping”, is commonly used to eliminate interferences. Beams may be coped at the top flange only, bottom flange only, or both the top and bottom flanges, depending on the connection geometry and layout. In situations where the supporting girder depth is larger than the beam depth, a single cope is required. Single copes typically involve the removal of the top—compression—flange of the beam. Double copes are required in situations where the girder and

¹ Master’s Student, University of Alberta, <gj1@ualberta.ca>

² Professor, University of Alberta, <rdriver@ualberta.ca>

³ Engineering Manager, Waiward Steel Fabricators, <logan.callele@waiward.com>

beam depths are equal. However, in both cases, special attention must be paid to the coped section due to the reduction in strength and torsional stiffness.

The end-support conditions of double-coped beams may differ. As such, there are options to connect the end of the coped section to the supporting element. A common method used in industrial construction—the method used in this research—is the use of a welded end-plate. The end-plate is typically shop welded to the coped web, then field bolted to the supporting element.

The behaviour of double-coped beam-to-girder connections differs if the connection is single-sided, *i.e.*, a beam framing into the girder from only one side of the girder web, shown schematically in Fig. 1(a), or symmetric, *i.e.*, a beam framing into the girder from both sides of the girder web, shown schematically in Fig. 1(b). The former case is likely to be used in an end bay, with little to no axial load in the supported beam. Gravity loads on the beam cause global deflection and twisting of the girder because the connection is asymmetric. Due to symmetry, the latter case will not exhibit global twisting of the girder if the beams on both sides are similarly loaded. If one beam is loaded more heavily than the other, the connection at the girder web can still provide twisting restraint to the girder web. Axial loads existing in supported beams arising from horizontal brace forces or diaphragm forces are considered to pass through, and so may exist in larger magnitudes compared to the case of a beam on one side only.

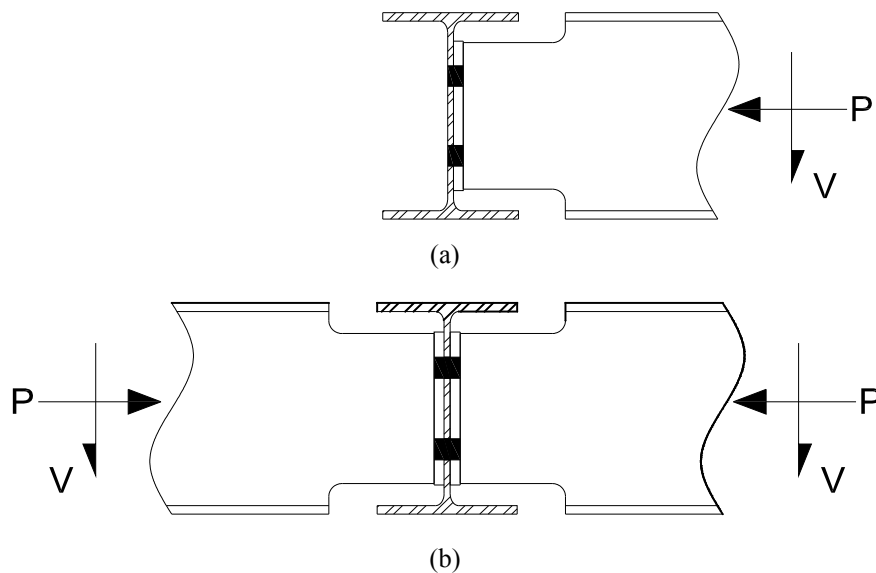


Figure 1: Combined loading on (a) beam on one side and (b) beam on both sides

2. Background

2.1. Previous Research

The predominant research done on coped connections was completed by Cheng *et al.* (1984); however, the experimental program of that research project focused on single-copes. Since then, some work has been completed into the investigation of local web buckling by Muir and Thornton (2004) and by Dowswell and Whyte (2013); however, no published information exists on the full-scale testing of double-coped beam-to-girder connections.

Cheng *et al.* (1984) noted the global lateral-torsional buckling strength of a coped beam is greatly reduced due to the removal of the flanges at the connection location. Typical lateral-torsional buckling strength formulations assume the beam ends are braced against rotation and lateral movement. Since the flanges have been removed at the supports, the beam remains susceptible to this failure mode. In typical construction practices, the structural elements would often be braced by the floor diaphragm or discrete bracing and so lateral-torsional buckling would not govern.

In a braced system, the extended single-plate at the reduced section becomes susceptible to local buckling. Depending on the application of load and the connection geometry, this may be flexural buckling or shear buckling, and the connection can be especially sensitive to the presence of axial loads. If the plate is long and has a slender cross-section, elastic buckling may occur before the section has yielded. If the plate is shorter with a thick web, local yielding may begin, followed by inelastic local web buckling. Re-entrant corners at the copes are areas of high stress concentration due to a geometric discontinuity, which can cause local yielding under bending before the section has reached its yield moment. After this area has yielded, stresses will continue to rise into the beam web, and inelastic buckling will occur. The localized yielding effect from the geometric discontinuity at the cope causes the assumed stress distributions from the traditional Mc/I and VQ/It equations for bending stress and shear stress to be invalid. In addition, the interaction between shear load, axial load, and moment on the coped section is complex. Despite the non-linear stress distributions across the coped section, many structural codes simply assume the distribution is linear, and the stress remains elastic, to simplify the design; however, this can often lead to overly conservative and costly connections.

2.2. Current Design Procedure

The Canadian Institute of Steel Construction Handbook of Steel Construction (CISC, 2010) provides design tables for situations where a single cope is required that have been experimentally shown to be conservative. The CISC Handbook outlines the design of end-plate connections; however, tables provided are restricted to non-coped beams. Although a double-coped beam connection is common in practice, the CISC Handbook gives no guidance to the designer.

The existing procedure in the American Institute of Steel Construction Steel Construction Manual (AISC, 2011) for determining the strength of coped beams is based on the available flexural local buckling strength of the coped section. The available strength is given as:

$$M_n = F_{cr} S_{net} \quad (1)$$

where F_{cr} is the flexural local buckling stress and S_{net} is the net section modulus at the face of the cope. The AISC procedure for determining the flexural local buckling stress for beams with the same cope length at both flanges was developed by Cheng *et al.* (1984). The flexural local buckling stress is based on a lateral-torsional buckling formulation with an adjustment factor to match finite element modelling results. The flexural local buckling stress is:

$$F_{cr} = 0.62\pi E \frac{t_w^2}{ch_0} f_d \leq F_y \quad (2)$$

where E is the modulus of elasticity, t_w is the thickness of the beam web, h_0 is the height of the coped section, c is the cope length, and f_d is an adjustment factor, as follows:

$$f_d = 3.5 - 7.5 \left(\frac{d_{ct}}{d} \right) \quad (3)$$

where d_{ct} is the cope depth at the compression flange, and d is the beam depth. The flexural local buckling stress is limited by the yield stress of the steel. Eq. 2 is only valid for $c \leq 2d$ and $d_c \leq d/2$, and does not include the effects of axial tension or compression. The available shear strength is calculated as:

$$V_n = M_n / e \quad (4)$$

where e is the load eccentricity, typically taken as the cope length plus the end-plate thickness, if applicable.

3. Scope and Objectives

The objective of this work is to conduct a number of full-scale tests of double-coped beam-to-girder connections. Due to the lack of previously published experimental data for this connection type, the primary focus of these tests is to contribute test data to the knowledge base. A secondary objective is to investigate the behaviour of the connections by determining the failure modes under combined loading—axial and shear—and determine the influencing parameters on that behaviour. Lastly, the suitability of currently used design practices will be assessed.

This research project has been separated into two phases: phase 1 connections are tested with an end condition similar to a symmetric scenario—the test specimens will connect to a rigid element with no rotation—and phase 2 connections are tested with an end condition similar to an asymmetric scenario—the test specimens will connect to a transverse girder. Of the 11 phase 1 tests planned, three have been completed at the time of writing this report, and so will be the focus herein.

4. Experimental Design

4.1. Test Set-up and Procedure

The test set-up for the phase 1 testing consisted of a stub column, a test specimen, a reusable beam, and three actuators, as shown in Fig. 2. Connections were tested using this system of three independent hydraulic actuators—two vertical actuators for shear load, one horizontal actuator for axial loads—to provide any ratio of shear and axial load to the connection. A reusable test beam connected the three hydraulic actuators to the double-coped specimens. All actuators were pinned at their ends to allow rotation during testing. Actuators were manually controlled in stroke-control with an air-driven hydraulic pump. The two vertical actuators used a steel baseplate and strong floor to react against, and the horizontal actuator used a reaction shear wall. In this set-up, the connection is loaded upwards.

Lateral supports were provided at two locations to prevent out-of-plane buckling under high compressive loads: at the vertical actuator closest to the coped section, and at the horizontal actuator. In both locations, lateral supports were provided on both sides of the beam. At the

vertical load actuator, bearing style supports were used with Teflon pads to reduce friction. At the horizontal load actuator, lateral support was provided with wheels to prevent friction. Electronic load cells and clinometers were mounted at each of the three actuators to calculate the total vertical and horizontal load applied to the connection. Beam rotation was monitored by an additional clinometer mounted to the beam web. Cable transducers were used to measure the stroke of each actuator, the distance from the test beam end-plate to the column stub, and the vertical displacement of the connection. The vertical displacement was measured from the steel floorplate to the bottom flange of the specimen at the beginning of the cope. At the connection interface, the end-plate tended to pull away from the column flange under tensile loads or under high vertical deflections of the test specimen. This end-plate displacement was measured by placing a tape measure in the field of view of a camera system, which took a series of photographs during each test. Following each test, the displacement was viewed and recorded manually. The camera system used was a non-contact deformation measurement tool that uses a pair of cameras to determine continuous strain contours on a 2D surface. In this instance, it was used to map the strain over the coped section during the tests.

The specimens were tested by first rotating the beam counter-clockwise (Fig. 2) to 0.03 radians, applying horizontal load, and then applying upward vertical load until failure occurs—maintaining the rotation and axial load. (Note that the beam is inverted as compared to in an actual structure resisting gravity load.) The rotation of 0.03 radians is commonly-used for testing shear connections, as it represents a typical beam end-rotation when the section has reached its full plastic capacity under a distributed load. Previous testing programs have shown that this value has little effect on the connection capacity; however, it is maintained to provide a level of accuracy to the overall behaviour of the connection. Failure was defined either by a sudden and significant decrease in vertical load, or after significant deformation of the connection, and at a point in which an increase in vertical displacement of the actuators results in further displacement of the connection with no additional load carrying capability.

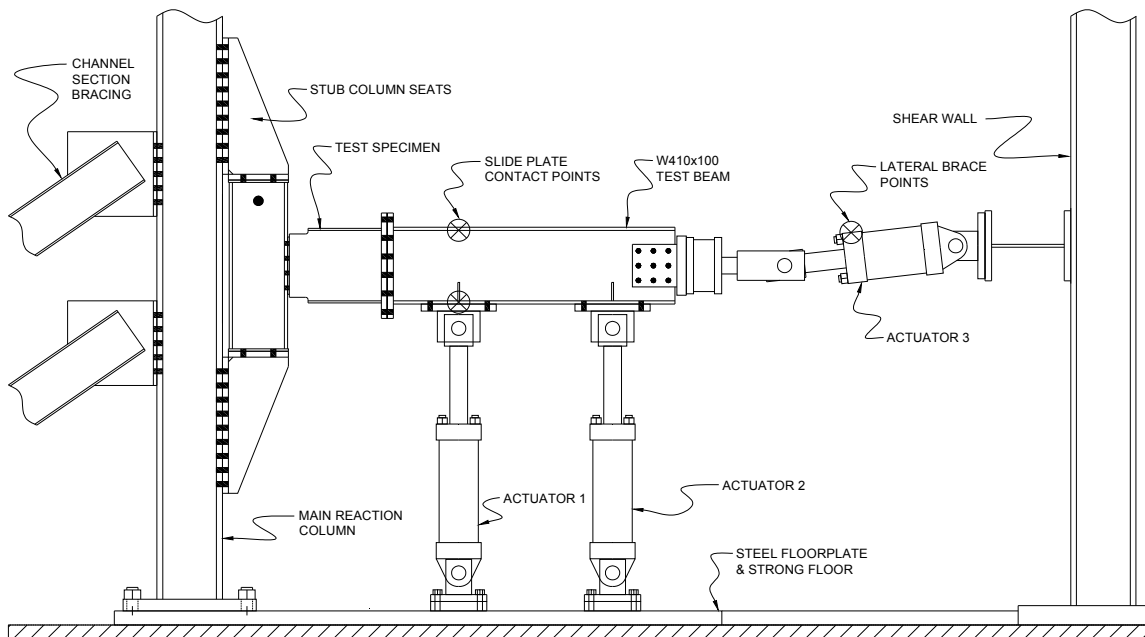


Figure 2: Test set-up

4.2. Specimen Design

The double-cope connections were designed based on the current procedures used at a local steel fabrication shop. Four test parameters will be investigated in this research: section depth, cope length, axial load, and support condition. However, the connections presented in this paper vary by axial load and cope length only.

Specimens were made from stub beams coped at one end only. The opposite end was used to connect the specimen to the test set-up. All specimens were coped at both top and bottom flanges—the cope depth and cope radius were 30 mm and 12.7 mm (1/2”), respectively, for all specimens. The cope depth, defined as the vertical distance from the outer face of the flange to the beam web at the cope, is used in this research is a standard value from the steel fabricator based on the required clearance in a typical beam-to-girder connection. The cope radius is the minimum to avoid potential stress concentrations at re-entrant corners, as recommended in the AISC Steel Construction Manual (AISC, 2011).

A four-variable alphanumeric identifier is used as the specimen designation for each connection. All three specimens tested were the same section—W200x27—and had the same end condition and geometry—a 9.5 mm (3/8”) thick end-plate fillet welded to both sides of the web, as shown in Fig. 3. The first two specimens tested, designated 2B-1-100C and 2B-1-100T, had the same cope length, 100 mm, shown in Fig. 4(a), but were loaded with 100 kN compression and 100 kN tension, respectively. The third specimen tested, designated 2B-3-0, had a 175 mm cope length, shown in Fig. 4(b), and was loaded in shear only, *i.e.*, horizontal load was kept at zero.

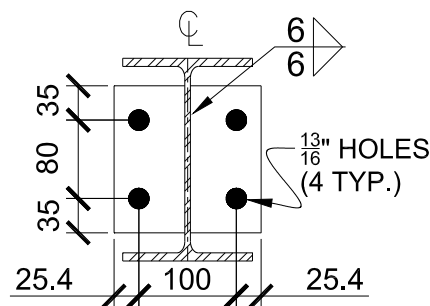


Figure 3: End-plate geometry

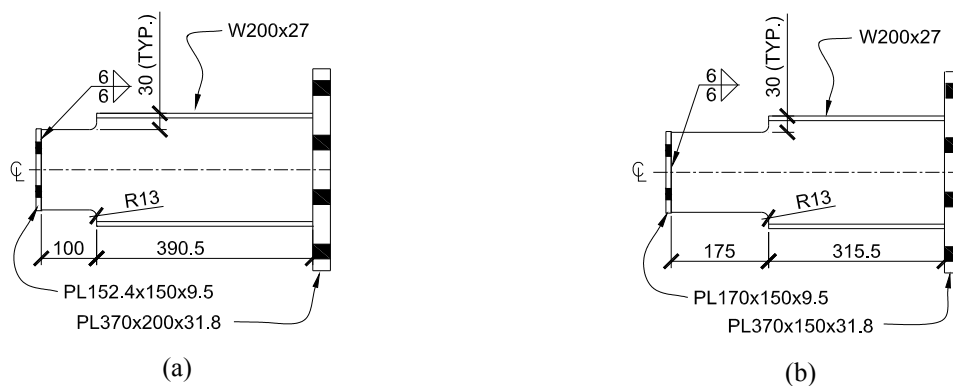


Figure 4: Specimen geometry for (a) 2B-1-100T & 2B-1-100C and (b) 2B-3-0

The remainder of the specimens to be tested in phase 1 and phase 2 of the testing program investigate the effect of section depth by comparing double copes on W200x27, W310x33, and W410x54 sections. These represent a typical range of sections suitable for double-coped connections. Larger shear and axial loads generally exceed the practical limits for this connection type, *e.g.*, if stiffeners are required, it is usually more cost effective to use a larger beam section or different connection type.

Three cope lengths are tested: 100 mm, 150 mm, and 175 mm. The minimum cope length used is the fabricator’s standard, based on minimum required clearance of these connection geometries. To avoid large capacity reductions from stability issues associated with long cope lengths, fabricators commonly detail copes at the minimum required length; however, larger cope lengths were tested because the stability of the web in the coped region is a main focus of this research project. In addition, long copes may be detailed in connections into a girder with a very wide flange, or in a skewed connection. By testing cope lengths larger than a practical maximum, the appropriateness of the equations governing the stability of the coped region can be determined.

The end-support conditions change in phase 2 of the research, as described previously. In addition, to determine if the end-plate connection has any significant effect on the connection capacity, stability, or ductility, connection tests are being completed with no end-plate, *i.e.*, the coped section is welded directly to the supporting element.

5. Experimental Results

The results from the three completed tests are summarized in Table 1. Details for each of the tests are given, in addition to the capacity predicted by the procedure outlined in Eqs. (1) to (4).

Table 1: Predicted and peak loads

Specimen ID	Axial Load Direction	Horizontal Load (kN)	Predicted Vertical Load (Eq. 4 ¹) (kN)	Peak Vertical Load (kN)
2B-1-100T	Tension	100	383	186
2B-1-100C	Compression	100	395	162
2B-3-0	-	0	123	138

¹ This method does not account for axial load. The predicted capacities of 2B-1-100T and 2B-1-100C differ due to the as-built measurements of the specimens.

Generally, the three specimens behaved in the same manner during the tests. Localized yielding began at the upper tip of the end-plate to web interface during the rotation phase. Following this, horizontal load was added, with no significant out-of-plane movement or yielding observed on any of the specimens. Vertical load was added, which resulted in a gradual rise in stress at the upper re-entrant corner due to the geometric discontinuity. In all specimens, the addition of vertical load created two vertical bands of high stress on the coped section: one at the weld toe at the end-plate, and one at the face of the cope. All three specimens developed their full plastic moment prior to their peak vertical load, as shown in the “von Mises strain” contours in Fig. 5. The contour scale, shown at the right, ranges from 0 to 10% strain. Note the higher strains associated with the specimens with higher capacity.

Following the peak vertical load, both 2B-1-100C and 2B-3-0 failed due to out-of-plane deformation and twisting of the cross-section, as shown in Figs. 6(b) and (c), respectively. 2B-1-100T did not display the same large out-of-plane deformations; it developed a tear at the base of the weld toe in the end-plate. As the tear propagated up the end-plate and the vertical load began to fall, a crack in the upper (tension side) re-entrant corner formed, as shown in Fig. 6(a). At this point, the vertical load dropped significantly and the test was ended.

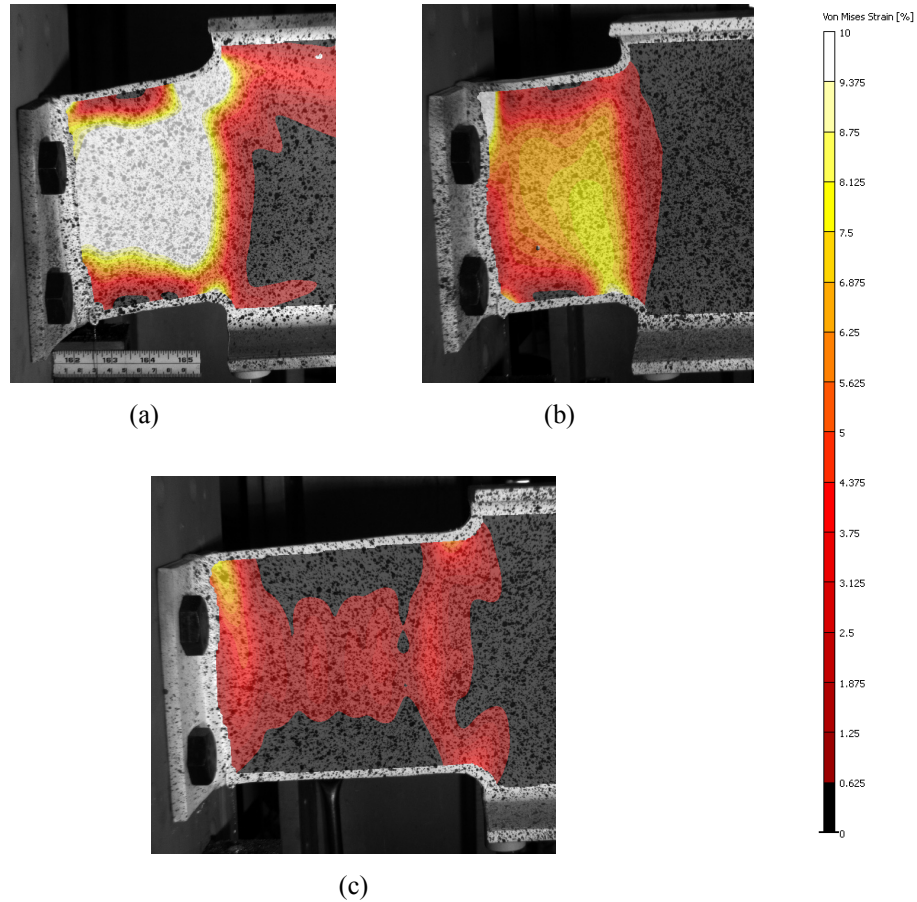


Figure 5: Von Mises strain at peak load for (a) 2B-1-100T, (b) 2B-1-100C, and (c) 2B-3-0

The behaviour of 2B-1-100T was shear-dominant. As the beam moved upwards under vertical load, the coped web angled downwards, developing a tension field along the diagonal. This high tension eventually caused the tear along the end-plate at the weld toe and the tear at the upper re-entrant corner.

The behaviour of 2B-1-100C and 2B-3-0 was also shear-dominant; however, these specimens failed by inelastic lateral-torsional buckling prior to the tension field developing to the point where a tear in the end-plate or the coped web could form. Lateral-torsional buckling of these specimens is evident in Figs. 6(b) and (c) as out-of-plane deformation and twisting of the cross-section.

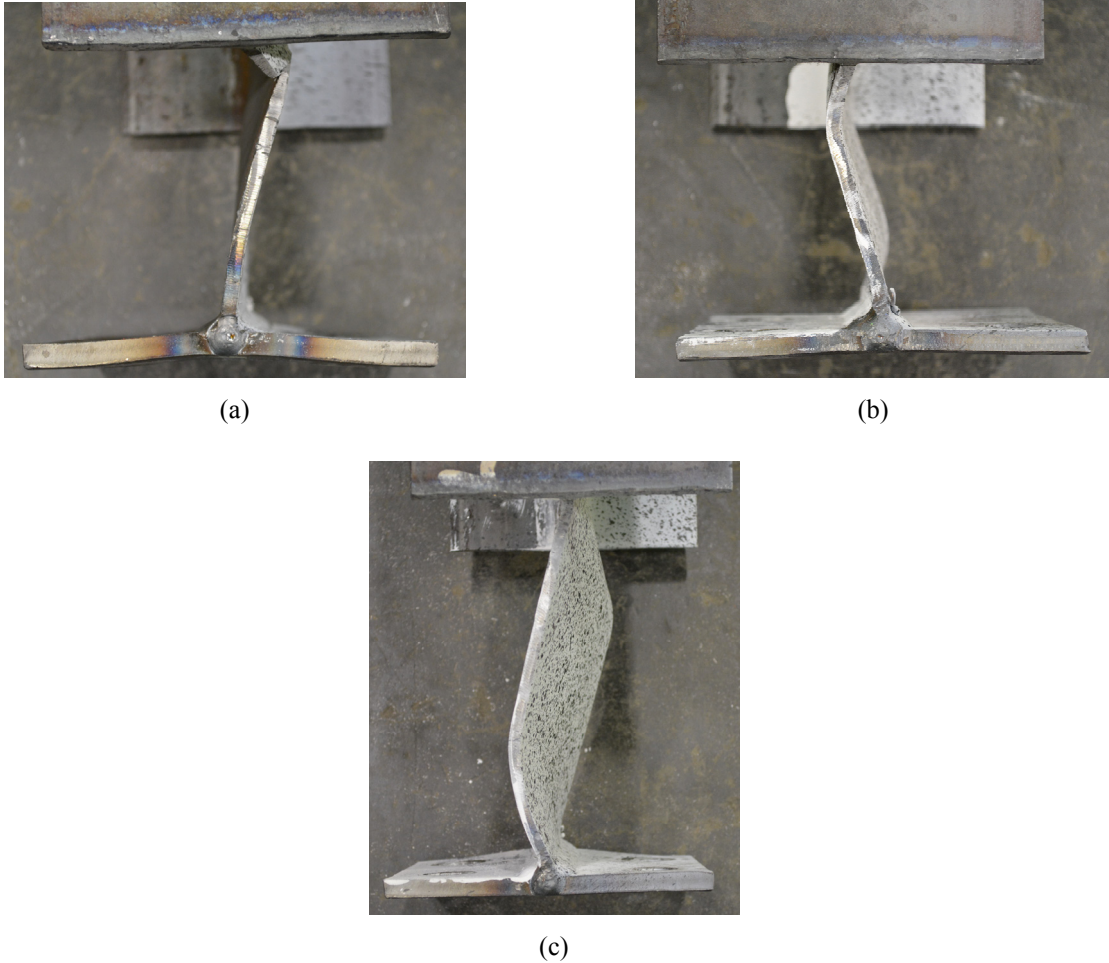


Figure 6: Deflected shapes for (a) 2B-1-100T, (b) 2B-1-100C, and (c) 2B-3-0

6. Influence of Key Variables

Figure 7 shows the vertical load vs. vertical displacement response curves for the three specimens tested. Under the rotation phase, all specimens undergo vertical displacement; however, the actuators are controlled so zero vertical load acts on the connection. This is shown in Fig. 7 as the period of zero vertical load at the beginning of each curve. For 2B-1-100C and 2B-1-100T, the rotation phase and horizontal load phases were complete at approximately 2.5 mm of vertical displacement, and for 2B-3-0, the rotation phase was complete at approximately 5.0 mm of vertical displacement.

Figure 8 shows the end-plate displacement at the bottom of the connection away from the stub column flange vs. vertical displacement curves for the three specimens tested. This displacement was limited to approximately the bottom 1/6 of the end-plate height—the majority of the end-plate remained in contact with the column flange for all tests. As expected, the greatest displacement of the end-plate away from the column flange occurred in the specimen loaded with axial tension. Due to the large vertical displacements, the other two connections also experienced separation of the end-plate from the column flange, even though compression was applied in the case of 2B-1-100C.

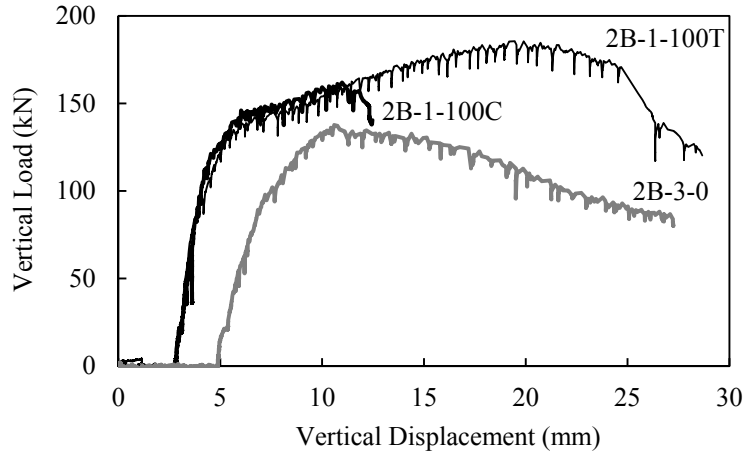


Figure 7: Vertical load vs. vertical displacement curves

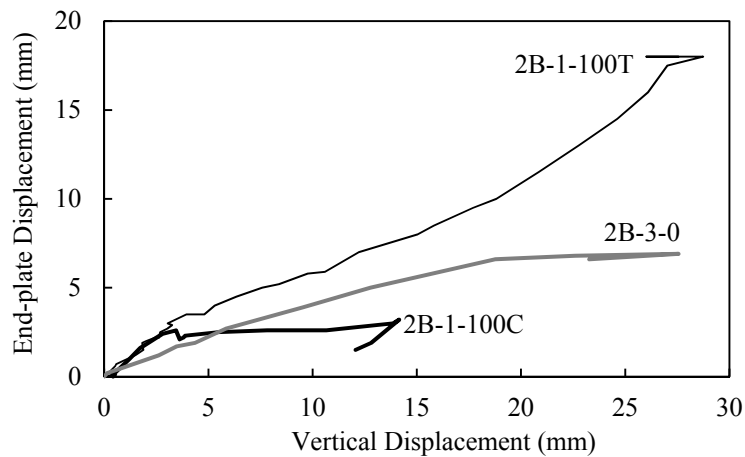


Figure 8: End-plate displacement vs. vertical displacement curves

6.1. Horizontal Load

The effect of compression on the connection is evident when comparing the load vs. displacement curves for specimens 2B-1-100T and 2B-1-100C—both the peak load and peak displacement are smaller for the compression-loaded specimen, as seen in Fig. 7. The peak vertical load of 2B-1-100T, 186 kN, is 24 kN greater, or 15%, than that of 2B-1-100C, 162 kN. The addition of tension to 2B-1-100T likely acted to stabilize the connection at high shear loads, allowing the specimen to develop a tension field. The ductility was also much higher; 2B-1-100T reached a displacement at the peak vertical load of 19.5 mm, compared to 11.0 mm for 2B-1-100C. At the failure, however, 2B-1-100C buckled and began to undergo significant deformation, while 2B-1-100T tore at the end-plate and the re-entrant corner. Note the similarities in the responses of these specimens up to the point where the compression specimen buckled. The connection behaviour does not appear to be sensitive to horizontal load in the elastic and initial inelastic ranges.

The effect of horizontal load is less clear in the load vs. displacement relationship when comparing either of the two tests with horizontal load to the shear-only test—2B-3-0—as this test also has a longer cope length. Unlike the specimens with a shorter cope length, 2B-3-0

experienced its peak vertical load immediately following the first, mostly linear portion of the curve. The initial stiffness of 2B-3-0 is very similar to that of the other specimens, indicating that horizontal load had little effect on these specimens' behaviours prior to yielding of the cross-section.

The effect of horizontal load is noted in Fig. 8 at approximately 2.5 mm vertical displacement for 2B-1-100T and 2B-1-100C—this is the point at which their behaviours begin to diverge. In 2B-1-100T, adding tension continues to pull the end-plate away from the column flange, and this trend increases non-linearly throughout the vertical load phase until failure. In 2B-1-100C, the introduction of compression is shown as a small decrease in end-plate displacement, as the end-plate is forced back towards the column, and does not significantly deform away from the column flange for the remainder of the test.

6.2. Cope Length

The increased cope length had an effect on the ductility of the 2B-3-0 connection. As shown in Fig. 7, under the initial application of vertical load, 2B-3-0 had similar stiffness; however, the overall ductility fell between that of the two other specimens, but the post-peak response was markedly more ductile than the specimens loaded with horizontal load, as the connection continued to deform with the application of vertical displacement. Due to the slenderness of the section, the increased cope length caused a decreased capacity—48 kN, or 26%, and 24 kN, or 15%—less than specimens 2B-1-100T and 2B-1-100C, respectively.

7. Summary and Conclusions

Double-coped beam-to-girder connections are a typical connection in steel framed buildings and a practical solution in eliminating interferences between members at the same elevation. However, there is no commonly adopted design procedure due to a lack of experimental testing on this connection type. Full-scale connection tests are underway at the University of Alberta to develop a better understanding of the behaviour of these connections.

The influences of two key variables on the behaviour of three double-coped beam-to-girder connections have been observed. The capacity of a double-coped connection is reduced when under the presence of axial compression due to buckling of the coped section prior to a tension field being formed. The presence of axial tension stabilizes the connection; however, after significant deformation, it may lead to brittle rupture. Double-coped connections with long cope lengths have a reduced capacity, and are more ductile in their post-peak response. More tests are needed to comment on the design assumptions used for these connections.

Acknowledgements

The authors thank Waiward Steel Fabricators for donating the test specimens. Financial support for this research was provided by the Natural Sciences and Engineering Research Council, the Steel Structures Education Foundation, and the University of Alberta.

References

- American Institute for Steel Construction (2011). *Steel Construction Manual*, 14th ed., AISC, Chicago, IL.
- Canadian Institute of Steel Construction. (2010). *Handbook of Steel Construction*. 10th ed., CISC, Markham, ON, Canada.
- Cheng, J.J., Yura, J.A., Johnson, C.P. (1984). "Design and Behavior of Coped Beam." Ferguson Lab Report, The University of Texas at Austin, Austin, TX.
- Dowswell, B., Whyte, R. (2013). "Localized Web Buckling of Double-Coped Beams." *Proceedings of the Annual Stability Conference*, Structural Stability Research Council, St. Louis, MO. 725-738.
- Muir, L.S., Thornton, W.A. (2004). "A Direct Method for Obtaining the Plate Buckling Coefficient for Double-Coped Beams." *Engineering Journal*, AISC, Third Quarter, Chicago, IL.